© 2019. Published by The Company of Biologists Ltd | Journal of Experimental Biology (2019) 222, jeb195750. doi:10.1242/jeb.195750

SHORT COMMUNICATION

Identification of a lipid-rich depot in the orbital cavity of the thirteen-lined ground squirrel

Amanda D. V. MacCannell[1,2,*], Kevin J. Sinclair[3], Glenn J. Tattersall[4], Charles A. McKenzie[3] and James F. Staples[1]

ABSTRACT

We discovered a previously undescribed orbital lipid depot in the thirteen-lined ground squirrel during the first ever magnetic resonance image (MRI) of this common experimental model of mammalian hibernation. In animals housed at constant ambient temperatures (5°C or 25°C, 12 h:12 h light:dark photoperiod), the volume of this depot increased in the autumn and decreased in the spring, suggesting an endogenous circannual pattern. Water-fat MRI revealed that throughout the year this depot is composed of ∼40% lipid, similar to brown adipose tissue (BAT). During arousal from torpor, thermal images showed higher surface temperatures near this depot before the rest of the head warmed, suggesting a thermoregulatory function. This depot, however, does not contain uncoupling protein 1, a BAT biomarker, or uncoupling protein 3. Histology shows blood vessels in close proximity to each other, suggesting it may serve as a vascular rete, perhaps to preferentially warm the eye and brain during arousals.

KEY WORDS: MRI, Hibernation, Adipose, Rete, *Ictidomys tridecemlineatus*, Orbit

INTRODUCTION

The thirteen-lined ground squirrel (*Ictidomys tridecemlineatus*) is a model organism for investigations of metabolic challenges that face hibernating mammals. The first published magnetic resonance image (MRI) of the thirteen-lined ground squirrel revealed the novel discovery of what appears to be a substantial depot of fatty tissue in the orbital cavity, located behind the eyes (MacCannell et al., 2017). We imaged this orbital lipid depot using the MRI pulse sequence iterative decomposition of water and fat with echo asymmetry and least-squares estimation (IDEAL), which quantifies the proton density fat fraction (PDFF), the fraction of tissue that is composed of lipid (Fuller et al., 2006; Reeder et al., 2005). The PDFF of brown adipose tissue (BAT) is known to be 30–70% (Hu et al., 2010; Rasmussen et al., 2013; Prakash et al., 2016), which is lower than that of white adipose tissue (WAT; 80–100%). We measured PDFF values of approximately 40% in this newly identified orbital depot (MacCannell et al., 2017).

We initially hypothesized that this lipid depot was one of several glands known to be located behind the eyes of other mammals, especially the Harderian gland (Wei Li, personal communication). In mice, lipid comprises approximately 35% of wet mass of the Harderian gland (Watanabe, 1980), close to the PDFF values we determined for this depot in ground squirrels. However, our preliminary investigations did not detect any porphyrin, a hallmark of the Harderian gland (Kennedy, 1970; Payne, 1994), within this orbital lipid depot. Moreover, we subsequently located the much smaller Harderian gland at the base of the optic nerve and confirmed its identity with a porphyrin assay. By contrast, this newly identified orbital lipid depot surrounds the optic nerve just posterior to the eye, and its nature remained unknown.

The PDFF values of this orbital lipid depot also closely resemble those of thorax BAT in ground squirrels (MacCannell et al., 2017). BAT has thermogenic capacity through the futile cycling of the electron transport system (ETS) caused by expression of uncoupling protein 1 (UCP1), which, when activated, allows protons pumped to the mitochondrial intermembrane space by the ETS to re-enter the mitochondrial matrix. In eutherian mammals, UCP1 is expressed predominately, if not exclusively, in BAT (Laursen et al., 2015), whereas other proteins in this family, such as UCP3, are expressed predominately in muscle (Raimbault et al., 2001). Owing to the MRI characteristics of this orbital lipid depot, we speculated that it might indeed be a BAT depot. Data from other mammalian hibernators supported this idea. Thermal images of hibernating bears show higher temperature around the eyes than the rest of the head (Laske et al., 2010). Also, Arctic ground squirrels (*Spermophilus parryii*) housed at −10°C showed a significantly higher brain temperature compared with the temperature of the liver, rectum, WAT and gastrocnemius muscle (Barger et al., 2006).

Hibernators have adapted to the thermal and energetic challenges of winter by undergoing seasonal hibernation, a strategy characterized by bouts of torpor that are spontaneously interrupted by periods of interbout euthermia (IBE). In Richardson's ground squirrels (*Urocitellus richardsonii*), entrance into torpor involves suppression of whole-animal metabolic rate, heart rate and body temperature (T_b) by 90%, 100-fold and 32°C, respectively (Wang, 1979). During arousal from torpor, BAT is activated, increasing both metabolic rate and T_b. In most mammals, including the thirteen-lined ground squirrel (MacCannell et al., 2017, 2019), BAT is located predominately within the thorax. We predict that if this orbital lipid depot is indeed BAT, then areas of the head near it may be warmer than other areas distal to thorax BAT depots during arousal. In most eutherian mammals, growth of BAT requires several days of exposure to decreased ambient temperature (T_a) (Nakamura and Morrison, 2007) or high-calorie diets (Rothwell and Stock, 1979). In hibernators, however, we (MacCannell et al., 2017) and others (Hindle and Martin, 2014) have found indications that BAT depots increase in size in the late summer and early autumn without cold exposure, suggesting regulation by an endogenous rhythm. If this cranial depot is indeed BAT, then we predict that it would show a pattern of growth similar to that of thoracic BAT, and would express UCP1.

[1]Department of Biology, University of Western Ontario, London, ON, N6A 5B8, Canada. [2]Discovery and Translational Science Department, University of Leeds, Leeds LS2 9DA, UK. [3]Department of Medical Biophysics, University of Western Ontario, London, ON, N6A 5B7, Canada. [4]Department of Biological Sciences, Brock University, St Catharines, ON, L2S 3A1, Canada.

*Author for correspondence (umamac@leeds.ac.uk)

A.D.V.M., 0000-0002-1294-5250

Received 26 November 2018; Accepted 16 January 2019

To our knowledge, our study (MacCannell et al., 2017) was the first to describe this orbital lipid depot, and there is no information about its properties or potential relevance for a hibernator. In the present study, we endeavoured to explore the structural and biochemical properties of this orbital lipid depot as well as its seasonal dynamics.

MATERIALS AND METHODS

Experimental animals

All procedures were approved by the University of Western Ontario Animal Care Committee (protocol 2012-016) and followed Canadian Council on Animal Care guidelines. Details of ground squirrel trapping and husbandry followed those we published recently (MacCannell et al., 2017).

For the MRI experiments, we used juvenile male thirteen-lined ground squirrels [*Ictidomys tridecemlineatus* (Mitchill 1821)] from the same litter that were housed at 22°C until weaning, after which they were divided randomly into two conditions: cold-housed (5°C) or warm-housed (thermoneutral; 25°C) (n=4 for each). After the initial MRI scan (see following section) of the cold-housed squirrels on 19 August 2016, T_a was decreased 1°C day^{-1} until it reached 5°C (6 September 2016). On 26 August 2016, immediately after the first MRI scan of the warm-housed animals, T_a was increased to 25°C. Both groups had a 12 h:12 h light:dark photoperiod. Rat chow (LabDiet 5P00), dry dog food (Iams) and water were provided *ad libitum*, with sunflower seeds and corn provided three times each week. Animals were weighed approximately once per week during cage changes; if animals were in torpor, cages were not changed so as to minimize disturbance. Torpor bouts were confirmed by the sawdust technique (Pengelley and Fisher, 1961), in which sawdust is placed on the back of a torpid squirrel and animals were observed daily for the presence of the sawdust. We use this technique because instrumenting these animals with T_b telemeters would have interfered with MRI.

Another group of squirrels that hibernated regularly were used for thermal imaging (see below). These animals were maintained at 22°C during the spring and summer (March until October), whereas during the winter months these animals were housed at 5°C. Details for housing can be found in Mathers et al. (2017).

MRI scanning

MRI was used to obtain T1-weighted images and IDEAL water-fat images from both cold- and warm-housed animals approximately every 3 weeks under isoflurane anaesthesia. The two treatment groups (cold- and warm-housed) were scanned on alternating weeks. MRI scanning details can be found in our recent publications (MacCannell et al., 2017, 2019).

Segmentation of MR images

Orbital lipid volume was segmented (i.e. outlined) using the OsiriX 5.6 (Bernex, Switzerland) 2D threshold region-growing algorithm tool, with segmentation parameters set to a lower threshold of 30% PDFF and an upper threshold of 70%, i.e. a minimum of 30% and a maximum of 70% of the tissue volume consisted of lipid, based on segmentation guidelines adapted from earlier studies on BAT from mice, rats and humans (Hu et al., 2010; Prakash et al., 2016; Rasmussen et al., 2013).

Immunoblot analysis

Both cold- and warm-housed animals were euthanized by anaesthetic overdose (Euthanyl, 54 mg 100 g^{-1}) following the final MRI scan, 1 year after the initial scan. Thorax BAT, orbital lipid depot, heart, gastrocnemius muscle and forebrain were dissected and stored at −80°C. These samples were homogenized in radioimmunoprecipitation assay (RIPA) buffer (50 mmol l^{-1} Tris, 150 mmol l^{-1} NaCl, 1% SDS, 0.5% sodium deoxycholate and 1% Triton X) for total protein extraction. Samples were centrifuged at 4°C and 10,000 ***g*** for 20 min before being stored at −80°C. Thirty micrograms of protein was separated by electrophoresis using 10% SDS–polyacrylamide gels. Gels were run at 180 V for 1 h in a running buffer (25 mmol l^{-1} Tris, 190 mmol l^{-1} glycine, 0.1% SDS), then transferred to polyvinylidene fluoride membranes. Transfer was conducted at 4°C at 100 V for 2 h. After transfer, membranes were blocked with 5% bovine serum albumin in Tris-buffered saline and Tween-20 (TBST; 30 mmol l^{-1} Tris, 137 mmol l^{-1} NaCl, 0.1% Tween-20, pH 7.6) under steady agitation for 2 h. Membranes were probed with a rabbit UCP1 antibody (primary antibody 1:1000; Abcam ab10983) or UCP3 primary antibody (1:1000 in TBST; Abcam, ab10985) overnight at 4°C. Rabbit anti-goat secondary (1:20,000; Abcam ab205718) was incubated for 1 h at room temperature under steady agitation. The membrane was washed three times for 10 min each in Tris-buffered saline and Tween-20 (TBST). Bands were visualized using Luminata Forte ECL (Millipore) using a VersaDoc MP5000 imaging system (BioRad). Bands were quantified using the densitometry analysis tool in ImageLab 3.0 (BioRad) and standardized to total protein in each lane, determined using Amido Black staining.

Statistical analyses

All values are presented as means±s.e.m. The effect of time, temperature or their interaction on PDFF or orbital lipid depot volume of cold- and warm-housed animals was assessed using a repeated-measures ANOVA and Greenhouse–Geisser correction in SPSS (IBM). Reliability of MRI segmentation volumes was confirmed by calculation of the interclass correlation coefficient (ICC) between values determined by A.D.V.M. and a second reader (P. Parthasarathy); ICC values higher than 0.9 indicate excellent reliability (Koo and Li, 2016).

CryoViz imaging

We used the CryoViz system to obtain visual images of this orbital lipid depot to confirm its corresponding position with MRI scans, and compare it visually with other tissues. One hibernating animal from a separate cohort (housed at 5°C, photoperiod 2 h:22 h light:dark) was euthanized by anaesthetic overdose on 29 November 2016 (euthanyl, 54 mg 100 g^{-1}) immediately following an IDEAL MRI. The squirrel was flash-frozen in optimal cutting temperature (OCT) freezing medium (Tissue-Tek® O.C.T. Compound, Sakura® Finetek) by liquid nitrogen immersion. The squirrel was sectioned sagitally every 50 µm and optical images were obtained using a cryo-fluorescence imager (CryoViz™; Bioinvision, Inc., Cleveland, OH, USA). Block-face images were collected with an in-plane resolution of 10.5×10.5 µm^2. Brightfield images were acquired, stitched together and visualized using proprietary software (Bioinvision, Inc.).

Histology

We conducted histology on BAT, orbital fat and WAT from cold- and warm-housed thirteen-lined ground squirrels. Tissues were removed immediately after euthanizing the animals, and were placed in 10% formalin for 24 h and then transferred to 70% ethanol until samples could be processed. Tissues were processed and embedded in paraffin wax blocks with a Leica ASP300 fully enclosed tissue processor. Hematoxylin & eosin (H&E) stain was applied using a

Journal of Experimental Biology (2019) 222, jeb195750. doi:10.1242/jeb.195750

Leica Autostainer XL. Tissues were processed and stained at the Western University Robarts Molecular Pathology Core Facility.

Imaging of the slides was conducted at the Biotron Integrated Microscopy, Western University, using a Zeiss Axioimager Z1 upright fluorescent/compound microscope.

Thermal imaging

Animals were removed from their cages in a lighted room and placed into a plastic container inside a small Styrofoam box that was cooled with icepacks, producing a T_a of approximately 7°C. Thermal imaging began within 1 min of removal of the cage from

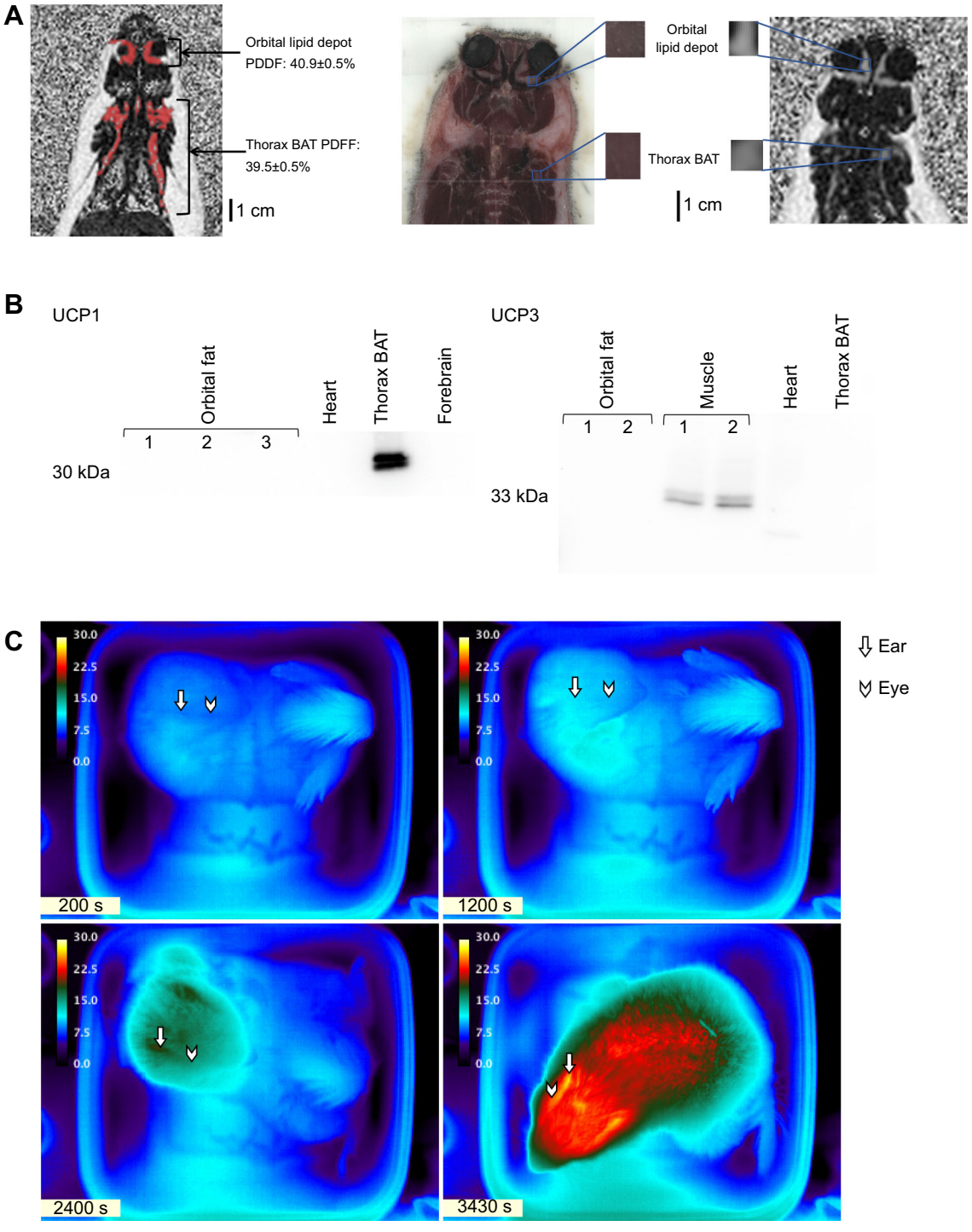

Fig. 1. Comparison of the orbital lipid depot with brown adipose tissue. (A) Proton density fat fraction (PDFF) magnetic resonance image (MRI) of a ground squirrel and CryoViz image of thorax. Example (left) of an MRI slice from a hibernating ground squirrel. Areas highlighted in red indicate location of PDFF values between 30–70%, expected values for BAT. The CryoViz image (centre) shows the orbital lipid depot corresponding precisely with the position of the tissue used for MRI analysis (right) and shows a close visual resemblance. (B) Immunoblots of uncoupling protein 1 (UCP1) and uncoupling protein 3 (UCP3) from various tissues of thirteen-lined ground squirrels. Numbers indicate different individuals from which the orbital lipid depot or skeletal muscle was sampled. (C) Thermal images of a squirrel during an induced arousal. Arrowhead indicates approximate location of the eye and the arrow indicates approximate location of the ear. Time stamps in the bottom left corner of images in C indicate elapsed time after removal from home cage.

the environment chamber. We induced arousal in 15 torpid ground squirrels that were hibernating at 5°C, 2 h:22 h light:dark photoperiod, by gentle agitation to their feet while in the Styrofoam container. We measured the surface temperature of these animals at 10 s intervals using a portable infrared thermal camera (model 7515, Mikron Instruments, Oakland, NJ, USA). Under these conditions, arousal to voluntary animal movement took, on average, 120 min, similar to the time course of spontaneous arousals in this species (MacCannell et al., 2018). To account for incident radiation, emissivity was set to 0.95 and the appropriate air temperature was used as the reflected temperature (reviewed in Tattersall, 2016). Thermal images were analyzed using commercial software (MikroSpec RT®, Mikron Instruments).

RESULTS & DISCUSSION

The PDFF of the orbital lipid depot was 40.9±0.5%, indistinguishable from that of BAT, with a PDFF of 39.5±0.5% (Fig. 1A). The CryoViz images correspond to the tissue used in biochemical analysis with the identified orbital lipid depot from the MRI (Fig. 1A). Visually, this orbital lipid depot also resembles BAT quite closely (Fig. 1A). Despite these apparent similarities between the orbital lipid depot and BAT, immunoblots did not detect any UCP1 in the orbital lipid depot (Fig. 1B), so the orbital lipid depot cannot be considered BAT. We did detect UCP1 in thoracic BAT, demonstrating strong reactivity with the rabbit-derived antibody. Moreover, we did not detect any UCP3 in the orbital lipid depot (Fig. 1B), or in heart or BAT, typical for these tissues (Raimbault et al., 2001). The lack of either UCP1 or UCP3 likely rules out any uncoupling thermogenic role for this orbital lipid depot. In recent years, the potential for non-shivering thermogenesis by skeletal muscle has received increasing research interest (reviewed by Rowland et al., 2015). Although this possibility is intriguing, the lack of UCP3 suggests that the orbital lipid does not originate from skeletal muscle (Boss et al., 1997), whereas ground squirrel skeletal muscle does show UCP3 reactivity (Fig. 1B).

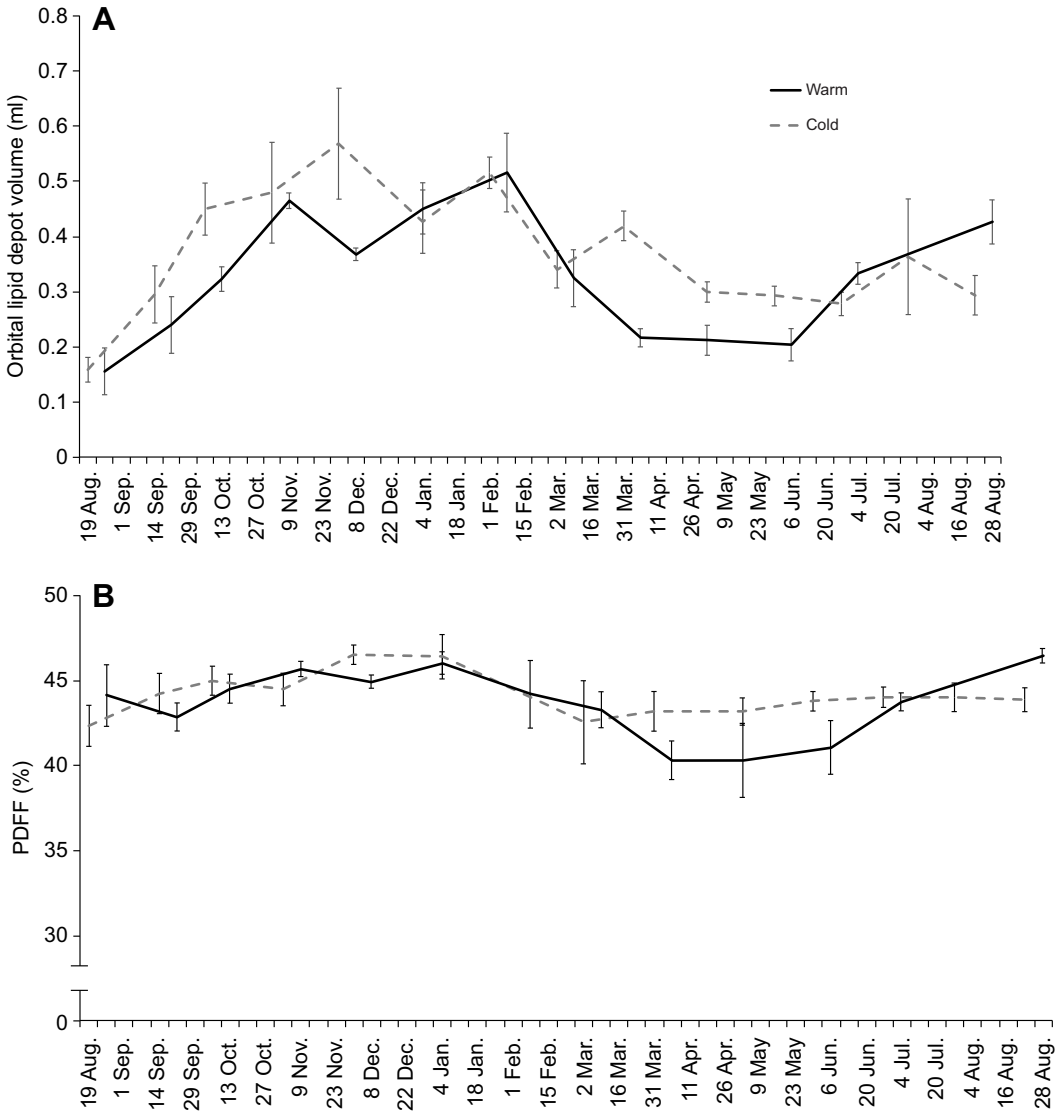

Fig. 2. Changes in the orbital lipid depot volume and lipid content. Volume of the orbital lipid depot over an entire year (A) and corresponding PDFF (B). The solid line represents animals housed at 25°C and the dashed line represents animals housed at 5°C. Both groups were housed under a 12 h:12 h light:dark photoperiod. Data are presented as means±s.e.m., n=4 for each group (repeated-measures ANOVA; eye fat volume: effect of time, $F_{3.0,18.2}$=10.9, P<0.001; temperature, $F_{1,6}$=1.7, P=0.25; time×temperature, $F_{3.0,18.2}$=2.4, P=0.11; PDFF: effect of time, $F_{2.6,15.5}$=3.7, P=0.051; temperature, $F_{1,6}$=0.3, P=0.6; time×temperature, $F_{2.6,15.5}$=1.5, P=0.3).

Journal of Experimental Biology (2019) 222, jeb195750. doi:10.1242/jeb.195750

Although we did not detect any potential for uncoupled thermogenesis in the orbital lipid depot, thermal images collected during arousals did show higher surface temperatures for the region near the eye and ear than for other parts of the head and thorax, suggesting greater heat loss in the head than in the thorax (Fig. 1C). Using these thermal images, we found that that the surface temperature near the eye increases at a higher rate than the thorax and feet (Movie 1, Fig. S1). The high surface temperature observed around the eyes indicates that this area is losing heat. This heat loss could be caused by lack of insulation or warm blood flowing to this area. Other fat depots, including WAT, are good insulators (Trayhurn and Beattie, 2001) and would reduce the rate of heat conduction to the external environment. The high heat loss leads us to believe that this orbital lipid depot is not functioning as an insulator.

The volume of the orbital lipid depot is dynamic, appearing to exhibit a circannual rhythm. Animals used in MRI experiments were housed under warm or cold conditions but under the same 12 h:12 h light:dark photoperiod. This design eliminated any overt seasonality cues within each group. Nonetheless, there was a significant effect of time ($F_{3.0,18.2}$=10.9, P<0.001), but not ambient temperature ($F_{1,6}$=1.7, P=0.3), on the volume of the orbital lipid depot. The orbital lipid depot of animals housed in constant cold and warm conditions started at 0.16±0.0 ml in late August but increased in size by a factor of 3.3 in both groups by early November (Fig. 2A). The depot size plateaued at 0.47±0.0 ml from November until early February before a 2-fold decrease, where the depot volume again levelled off at 0.25±0.0 ml in May. After a full year, the orbital depot was 0.36±0.0 ml in both groups, 2.3-fold greater than the original volume in August 2016. The PDFF of the orbital lipid depot did not vary significantly over time or between the two groups ($F_{2.6,15.5}$=1.5, P=0.26), remaining fairly constant near 43% (Fig. 2B). The consistent PDFF indicated that there is no change in the water to fat ratio of the depot despite the changes in depot volume. If this orbital lipid depot was one of the glands commonly found near mammal eyes (Harderian, Meibomian or lacrimal), we cannot conceive of a hypothesis that would address why its volume would vary 3-fold over the course of a year. Indeed, in rats, the mass of the lacrimal gland, located within the orbit, increases linearly following birth, but plateaus at an age of 100 days, without further dramatic changes in size over the lifetime of the animal (Walker, 1958).

H&E staining of BAT showed the well-documented pattern of multivacuolated lipid droplets, while WAT showed univacuolated lipid droplets, typical for these tissues (George and Eapen, 1959) (Fig. 3A,B). In contrast, the orbital lipid depot appears to have multi-layered cuboidal epithelial cells surrounding what resemble blood vessels (Fig. 3C). These distinct patterns allow us to conclude that the eye fat depot does not consist of WAT or BAT. In fact, the presence of blood vessels in close apposition is reminiscent of a vascular rete. H&E staining of a swine rete mirabile located at the skull base within the cavernous sinuses shows similarities to the ground squirrel orbital lipid depot in terms of cell type, size and proximity of blood vessels (Arakawa et al., 2007).

The dynamic volume changes, increased regional temperature, lack of UCPs and high level of vascularization lead us to hypothesize that this tissue might be a rete, a network of many arterial and venous blood vessels in close proximity to each other, creating a counter-current pattern of blood flow (Cech et al., 1984). Such structures are found within several different taxa including birds, fish and mammals, with some retia located near the eyes and orbital sinuses of salmon sharks and bigeye thresher sharks, where

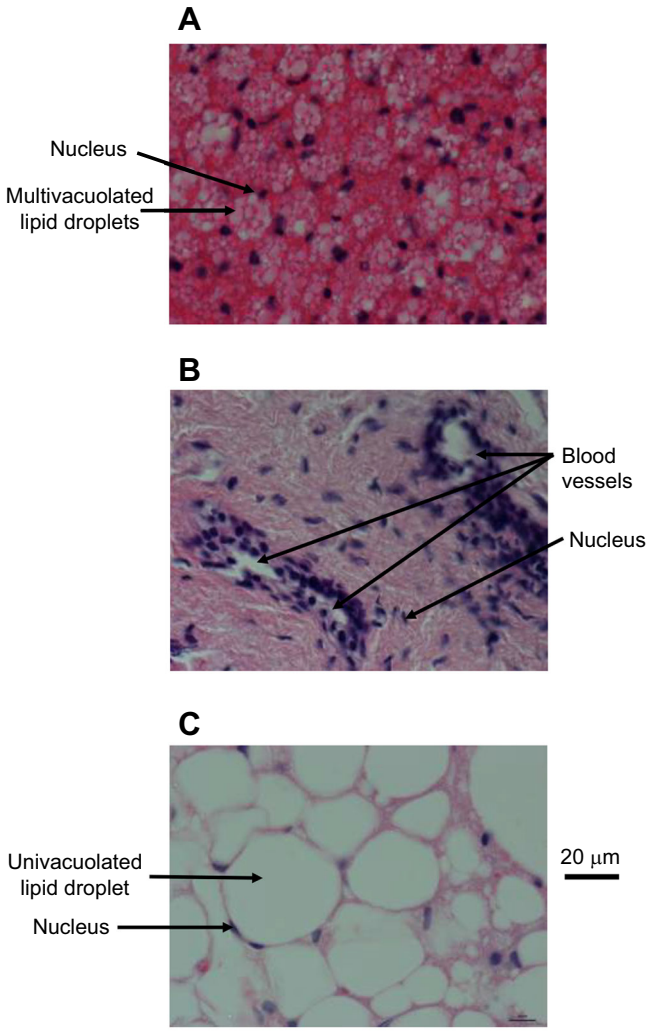

Fig. 3. Hematoxylin & eosin staining of tissues of thirteen-lined ground squirrels. (A) Brown adipose tissue; (B) orbital fat; and (C) white adipose tissue. Tissues were formalin fixed and paraffin embedded. Sectioning shows distinct variations in histology of the tissues. All photomicrographs are shown with the same magnification; scale bar indicates 20 μm.

they appear to function as vascular heat exchangers (Cech et al., 1984; Weng and Block, 2004). In these animals, such counter-current heat exchange restricts heat loss across the surface of the eyes, while presumably warming the nearby brain. Such a mechanism may have been advantageous during the evolution of hibernators such as thirteen-lined ground squirrels. In this species, hibernation occurs in burrows below the frost line. These animals arouse from torpor spontaneously approximately every 12 days throughout the winter. During arousal, metabolic rate and ventilation rate increase substantially (Wang, 1979). The increased rate of intake of cold air through the nasal cavities during arousal could constrain the rate at which the nearby eyes and brain could rewarm, and there is little insulation in this region. Most of the heat generated during the early stages of an arousal is derived from BAT, but BAT is concentrated deep within the thorax, and this heat is delivered convectively to other body regions through the blood. In fact, during the early stages of arousal in hamsters, blood flow is restricted to the thorax and head (Osborne et al., 2005). As this warm blood reaches the periphery of the head, a rete would reduce loss of heat from warmed blood to the environment through

this poorly insulated region. This suggestion is supported by our thermal images; the increase in temperature observed around the eyes could result from warm blood flowing from the thorax and being retained in the region by the rete. The brain plays a major role in regulating changes to T_b, metabolism and several physiological variables during arousal in other hibernators including the golden-mantled ground squirrel (Heller and Colliver, 1974; Dark et al., 1990), so rewarming of the brain before other tissues would likely be advantageous. To our knowledge, however, such an orbital lipid depot has not been reported in other hibernators, but brain temperature is higher during torpor at a T_a of −10°C in Arctic ground squirrels (Barger et al., 2006), and Columbian ground squirrels warm up their brains before their body after return to normoxia from hypoxia (Tattersall and Milsom, 2009). Both of these observations could be explained by a rete acting as a head-specific heat retention organ.

To confirm that this orbital lipid depot is a rete mirable, a 'wonderful network' of blood vessels, we propose using the powerful technique of differential-contrast, dual-vascular injection (DICOM) with X-ray microcomputed tomography (micro CT). This method has been used recently to characterize sites of heat exchange within bird heads (Porter and Witmer, 2016). If confirmed, this discovery would, to our knowledge, be the first ever documented rete in the orbital cavity of a mammal.

Acknowledgements
We thank Lauren Smith and Stephanie Giza for MRI scanning assistance. We thank Prasiddah Parthasarathy for being a second reader for MRIs and Alirezaa Akbari for assistance with reconstruction of MRIs. We thank the University of Western Ontario Biotron for use of microscope, training and support. Also, we thank the Robarts pathology lab for histology, Christopher Guglielmo for input and ideas on this project and Amanda Hamilton for help with the CryoViz. We thank Kate Mathers, Leah Hayward and Xingyi Wang for their animal care support.

Competing interests
The authors declare no competing or financial interests.

Author contributions
Conceptualization: A.D.M., J.F.S.; Methodology: A.D.M., G.J.T.; Software: K.J.S., G.J.T.; Validation: A.D.M.; Formal analysis: A.D.M., G.J.T.; Investigation: A.D.M., K.J.S.; Resources: G.J.T., C.A.M., J.F.S.; Writing - original draft: A.D.M.; Writing - review & editing: A.D.M., K.J.S., G.J.T., C.A.M., J.F.S.; Visualization: A.D.M., G.J.T., J.F.S.; Supervision: C.A.M., J.F.S.; Funding acquisition: C.A.M., J.F.S.

Funding
This research was supported by Discovery Grants from the Natural Sciences and Engineering Research Council of Canada (RGPIN-2013-356310 to C.A.M.; RGPIN-2014-05814 to G.J.T.; and RGPIN-2014-04860 to J.F.S.), the Faculty of Science, University of Western Ontario, and the Canada Research Chairs program (950-228038 to C.A.M.).

Supplementary information
Supplementary information available online at
http://jeb.biologists.org/lookup/doi/10.1242/jeb.195750.supplemental

References
Arakawa, H., Murayama, Y., Davis, C. R., Howard, D. L., Baumgardner, W. L., Marks, M. P. and Do, H. M. (2007). Endovascular embolization of the swine rete mirabile with eudragit-E 100 polymer. *Am. J. Neuroradiol.* **28**, 1191-1196.

Barger, J. L., Barnes, B. M. and Boyer, B. B. (2006). Regulation of UCP1 and UCP3 in arctic ground squirrels and relation with mitochondrial proton leak. *J. Appl. Physiol.* **101**, 339-347.

Boss, O., Samec, S., Paoloni-Giacobino, A., Rossier, C., Dulloo, A., Seydoux, J., Muzzin, P. and Giacobino, J.-P. (1997). Uncoupling protein-3: a new member of the mitochondrial carrier family with tissue-specific expression. *FEBS Lett.* **408**, 39-42.

Cech, J. J., Laurs, R. M. and Graham, J. B. (1984). Temperature-induced changes in blood gas equilibria in the albacore, *Thunnus alalunga*, a warm-bodied tuna. *J. Exp. Biol.* **109**, 21-34.

Dark, J., Kilduff, T. S., Heller, H. C., Licht, P. and Zucker, I. (1990). Suprachiasmatic nuclei influence hibernation rhythms of golden-mantled ground squirrels. *Brain Res.* **509**, 111-118.

Fuller, S., Reeder, S., Shimakawa, A., Yu, H., Johnson, J., Beaulieu, C. and Gold, G. E. (2006). Iterative decomposition of water and fat with echo asymmetry and least-squares estimation (IDEAL) fast spin-echo imaging of the ankle: initial clinical experience. *Am. J. Roentgenol.* **187**, 1442-1447.

George, J. C. and Eapen, J. (1959). A histological and histochemical study of the brown and yellow adipose tissue of the bat, *Hipposideros speoris*. *J. Cell Sci.* **51**, 369-375.

Heller, H. C. and Colliver, G. W. (1974). CNS regulation of body temperature during hibernation. *Am. J. Physiol. Leg. Content* **227**, 583-589.

Hindle, A. G. and Martin, S. L. (2014). Intrinsic circannual regulation of brown adipose tissue form and function in tune with hibernation. *Am. J. Physiol. Endocrinol. Metab.* **306**, E284-E299.

Hu, H. H., Smith, D. L., Nayak, K. S., Goran, M. I. and Nagy, T. R. (2010). Identification of brown adipose tissue in mice with fat-water IDEAL-MRI. *J. Magn. Reson. Imaging JMRI* **31**, 1195-1202.

Kennedy, G. Y. (1970). Harderoporphyrin: a new porphyrin from the Harderian glands of the rat. *Comp. Biochem. Physiol.* **36**, 21-36.

Koo, T. K. and Li, M. Y. (2016). A guideline of selecting and reporting intraclass correlation coefficients for reliability research. *J. Chiropr. Med.* **15**, 155-163.

Laske, T. G., Harlow, H. J., Garshelis, D. L. and Iaizzo, P. A. (2010). Extreme respiratory sinus arrhythmia enables overwintering black bear survival–physiological insights and applications to human medicine. *J. Cardiovasc. Transl. Res.* **3**, 559-569.

Laursen, W. J., Mastrotto, M., Pesta, D., Funk, O. H., Goodman, J. B., Merriman, D. K., Ingolia, N., Shulman, G. I., Bagriantsev, S. N. and Gracheva, E. O. (2015). Neuronal UCP1 expression suggests a mechanism for local thermogenesis during hibernation. *Proc. Natl. Acad. Sci. USA* **112**, 1607-1612.

MacCannell, A., Sinclair, K., Friesen-Waldner, L., McKenzie, C. A. and Staples, J. F. (2017). Water–fat MRI in a hibernator reveals seasonal growth of white and brown adipose tissue without cold exposure. *J. Comp. Physiol. B* **187**, 759-767.

MacCannell, A. D. V., Jackson, E. C., Mathers, K. E. and Staples, J. F. (2018). An improved method for detecting torpor entrance and arousal in a mammalian hibernator using heart rate data. *J. Exp. Biol.* **221**, jeb174508.

MacCannell, A. D. V., Sinclair, K. J., McKenzie, C. A. and Staples, J. F. (2019). Environmental temperature effects on adipose tissue growth in a hibernator. *J. Exp. Biol.* **222**, jeb194548.

Mathers, K. E., McFarlane, S. V., Zhao, L. and Staples, J. F. (2017). Regulation of mitochondrial metabolism during hibernation by reversible suppression of electron transport system enzymes. *J. Comp. Physiol. B* **187**, 227-234.

Nakamura, K. and Morrison, S. F. (2007). Central efferent pathways mediating skin cooling-evoked sympathetic thermogenesis in brown adipose tissue. *Am. J. Physiol. Regul. Integr. Comp. Physiol.* **292**, R127-R136.

Osborne, P. G., Sato, J., Shuke, N. and Hashimoto, M. (2005). Sympathetic α-adrenergic regulation of blood flow and volume in hamsters arousing from hibernation. *Am. J. Physiol. Regul. Integr. Comp. Physiol.* **289**, R554-R562.

Payne, A. P. (1994). The harderian gland: a tercentennial review. *J. Anat.* **185**, 1-49.

Pengelley, E. T. and Fisher, K. C. (1961). Rhythmical arousal from hibernation in the golden-mantled ground squirrel, *Citellus lateralis tescorum*. *Can. J. Zool.* **39**, 105-120.

Porter, W. R. and Witmer, L. M. (2016). Avian cephalic vascular anatomy, sites of thermal exchange, and the rete ophthalmicum. *Anat. Rec.* **299**, 1461-1486.

Prakash, K. N. B., Verma, S. K., Yaligar, J., Goggi, J., Gopalan, V., Lee, S. S., Tian, X., Sugii, S., Leow, M. K. S., Bhakoo, K. et al. (2016). Segmentation and characterization of interscapular brown adipose tissue in rats by multi-parametric magnetic resonance imaging. *Magn. Reson. Mater. Phys. Biol. Med.* **29**, 277-286.

Raimbault, S., Dridi, S., Denjean, F., Lachuer, J., Couplan, E., Bouillaud, F., Bordas, A., Duchamp, C., Taouis, M. and Ricquier, D. (2001). An uncoupling protein homologue putatively involved in facultative muscle thermogenesis in birds. *Biochem. J.* **353**, 441-444.

Rasmussen, J. M., Entringer, S., Nguyen, A., van Erp, T. G. M., Guijarro, A., Oveisi, F., Swanson, J. M., Piomelli, D., Wadhwa, P. D., Buss, C. et al. (2013). Brown adipose tissue quantification in human neonates using water-fat separated MRI. *PLoS ONE* **8**, e77907.

Reeder, S. B., Pineda, A. R., Wen, Z., Shimakawa, A., Yu, H., Brittain, J. H., Gold, G. E., Beaulieu, C. H. and Pelc, N. J. (2005). Iterative decomposition of water and fat with echo asymmetry and least-squares estimation (IDEAL): application with fast spin-echo imaging. *Magn. Reson. Med.* **54**, 636-644.

Rothwell, N. J. and Stock, M. J. (1979). A role for brown adipose tissue in diet-induced thermogenesis. *Nature* **281**, 31.

Rowland, L. A., Bal, N. C. and Periasamy, M. (2015). The role of skeletal-muscle-based thermogenic mechanisms in vertebrate endothermy. *Biol. Rev.* **90**, 1279-1297.

Tattersall, G. J. (2016). Infrared thermography: a non-invasive window into thermal physiology. *Comp. Biochem. Physiol. A. Mol. Integr. Physiol.* **202**, 78-98.

Tattersall, G. J. and Milsom, W. K. (2009). Hypoxia reduces the hypothalamic thermogenic threshold and thermosensitivity. *J. Physiol.* **587**, 5259-5274.
Trayhurn, P. and Beattie, J. H. (2001). Physiological role of adipose tissue: white adipose tissue as an endocrine and secretory organ. *Proc. Nutr. Soc.* **60**, 329-339.
Walker, R. (1958). Age changes in the rat's exorbital lacrimal gland. *Anat. Rec.* **132**, 49-69.
Wang, L. C. H. (1979). Time patterns and metabolic rates of natural torpor in the Richardson's ground squirrel. *Can. J. Zool.* **57**, 149-155.
Watanabe, M. (1980). An autoradiographic, biochemical, and morphological study of the Harderian gland of the mouse. *J. Morphol.* **163**, 349-365.
Weng, K. C. and Block, B. A. (2004). Diel vertical migration of the bigeye thresher shark (*Alopias superciliosus*), a species possessing orbital retia mirabilia. *Fish. Bull.* **102**, 221-229.